Molecular Ultrasound Imaging of Junctional Adhesion Molecule A Depicts Acute Alterations in Blood Flow and Early Endothelial Dysregulation

Adelina Curaj, Zhuojun Wu, Anne Rix, Oliver Gresch, Marieke Sternkopf,
Setareh Alampour-Rajabi, Twan Lammers, Marc van Zandvoort, Christian Weber,
Rory R. Koenen, Elisa A. Liehn,* Fabian Kiessling*

Objective—The junctional adhesion molecule A (JAM-A) is physiologically located in interendothelial tight junctions and focally redistributes to the luminal surface of blood vessels under abnormal shear and flow conditions accompanying atherosclerotic lesion development. Therefore, JAM-A was evaluated as a target for molecularly targeted ultrasound imaging of transient endothelial dysfunction under acute blood flow variations.

Approach and Results—Flow-dependent endothelial dysfunction was induced in apolipoprotein E–deficient mice (n=43) by carotid partial ligation. JAM-A expression was investigated by molecular ultrasound using antibody-targeted poly(n-butyl cyanoacrylate) microbubbles and validated with immunofluorescence. Flow disturbance and arterial remodeling were assessed using functional ultrasound. Partial ligation led to an immediate drop in perfusion at the ligated side and a direct compensatory increase at the contralateral side. This was accompanied by a strongly increased JAM-A expression and JAM-A–targeted microbubbles binding at the partially ligated side and by a moderate and temporary increase in the contralateral artery (≈14× [$P<0.001$] and ≈5× [$P<0.001$] higher than control, respectively), both peaking after 2 weeks. Subsequently, although JAM-A expression and JAM-A–targeted microbubbles binding persisted at a higher level at the partially ligated side, it completely normalized within 4 weeks at the contralateral side.

Conclusions—Temporary blood flow variations induce endothelial rearrangement of JAM-A, which can be visualized using JAM-A–targeted microbubbles. Thus, JAM-A may be considered as a marker of acute endothelial activation and dysfunction. Its imaging may facilitate the early detection of cardiovascular risk areas, and it enables the therapeutic prevention of their progression toward an irreversible pathological state.

Visual Overview—An online visual overview is available for this article. (*Arterioscler Thromb Vasc Biol*. 2018;38:40-48. DOI: 10.1161/ATVBAHA.117.309503.)

Key Words: atherosclerosis ■ cell adhesion molecules ■ ligation ■ microbubbles ■ molecular imaging

Atherosclerosis is a leading cause of morbidity and mortality in the Western world. The initial hallmark of atherosclerotic lesion development is endothelial dysfunction, and one of the main triggers is luminal flow alteration.[1] As a result, vessel bifurcations and vessel curvatures[2] are predilection sites for the development of lesions because of natural disturbance of laminar flow. Here, molecular changes in the endothelium may indicate whether alterations in perfusion are of pathological relevance.[3,4] Therefore, the identification of specific early stage biomarkers in combination with an easy accessible, radiation-free, noninvasive, and cheap diagnostic method is of high importance.

An increased risk of plaque development is associated with elevated serum levels of circulating cytokines, such as tumor necrosis factor-α, interleukin-6, and C-reactive protein. However, these are unspecific disease markers elevated in multiple pathologies and therefore cannot be used for specific diagnosis of early atherosclerosis. Consequently, monitoring the upregulation of membrane-bound surface adhesion molecules, like cell adhesion molecules and selectins,[5] by molecular imaging techniques represents a promising approach. In the past decade, advances in molecular targeting of endothelial lesions in big and small arteries have been achieved using

DOI: 10.1161/ATVBAHA.117.309503

Nonstandard Abbreviations and Acronyms	
JAM-A	junctional adhesion molecule A
MB$_{JAM-A}$	JAM-A–targeted microbubbles

different diagnostic probes recognizing activated endothelial cells, such as targeted phospholipid-based micelles[6] for magnetic resonance imaging and ligand-modified microbubbles[7,8] for molecular ultrasound imaging. Molecular ultrasound was introduced as an extension of conventional ultrasound imaging,[9] which is capable of quantifying flow velocity and back flow within major arteries, providing anatomic and functional data, but which lacks information at the molecular level.[10] Prominent inflammation biomarkers, such as intercellular adhesion molecule 1,[11] vascular cell adhesion molecule 1,[7,8,12] P-selectin,[13] and $\alpha_v\beta_3$,[14] have already been evaluated for molecular diagnosis of different stages of atherosclerosis[15–18] by using targeted radiotracers,[6] liposomes,[19] and microbubbles.[8] However, early detection of active endothelial sites remains challenging for many targets because of their constitutive luminal availability,[11,20,21] transient upregulation,[11,20,21] target access,[22,23] or partial solubility.[24] Therefore, consensus toward the clinical translation has not yet been found.[25]

Nevertheless, junctional adhesion molecule A (JAM-A) has been recently involved in molecular imaging protocols using targeted ultra-small iron oxide particles nanoparticles and microbubbles.[26] JAM-A proved to be the biological marker most responsive to acute changes in blood flow,[27] being upregulated specifically on endothelial cells at the flow-dependent predilection sites of atherosclerosis,[28] which are responsible for monocyte recruitment and accumulation in the vascular wall.[27] Junctional adhesion molecules are members of an immunoglobulin subclass, which under nonpathological conditions are located in the tight junctions of endothelial and epithelial cells,[29] inaccessible from the lumen. Recent studies have shown redistribution of JAM-A to the luminal surface consequent to inflammatory stimuli and endothelial activation and have uncovered a pivotal role for JAM-A in leukocyte recruitment and transmigration.[30,31] Furthermore, it was found that the knockout of endothelial JAM-A impairs leukocyte migration and confers atheroprotective effects.[30] JAM-A has an important role in leukocyte recruitment on early atherosclerotic endothelium,[30] by supporting endothelial deposition of CC-chemokine ligand 5 from activated platelets.[31] It also modulates the function of C-X-C-chemokine receptor type 4–bearing hematopoietic stem cells by direct interaction.[32] Both facts support the suggestion of JAM-A as an early atherosclerotic lesion marker.

The aim of our study was to evaluate JAM-A as a target for molecular ultrasound imaging of transient endothelial activation under acute blood flow variations. Therefore, we used JAM-A–targeted poly(n-butyl cyanoacrylate) microbubbles (MB$_{JAM-A}$) as a contrast agent for molecular ultrasound imaging in a mouse model of flow-induced endothelial activation followed by atherosclerotic plaque development. We found that MB$_{JAM-A}$ bound specifically to JAM-A on activated endothelium and were able to identify the location of areas with endothelial dysfunction. Furthermore, our data show that not only flow reduction because of vessel obstruction but also

flow increase because of compensatory blood flow redistribution in the contralateral carotid induce luminal exposure of JAM-A, both illustrating the high sensitivity of this marker for assessing acute vascular vulnerability and remodeling.

Materials and Methods

Materials and Methods are available in the online-only Data Supplement.

Results

Analysis of the Binding Affinity of MB$_{JAM-A}$ In Vitro

The number of bound microbubbles was determined using fluorescence microscopy (Figure 1A–1E), showing that MB$_{JAM-A}$ bound ≈7× more ($P<0.0001$) to stimulated human aortic endothelial cells than to unstimulated cells (Figure 1F) and ≈7× more ($P<0.0001$) than nontargeted control microbubbles. There was no significant difference between the binding efficiency of control nontargeted microbubbles (Figure 1F) and MB$_{JAM-A}$ on unstimulated human aortic endothelial cells, showing the binding specificity of the MB$_{JAM-A}$. Moreover, the binding specificity of MB$_{JAM-A}$ was confirmed by the competitive binding studies (Figure 1F).

Molecular Ultrasound Imaging of JAM-A Expression in Carotid Arteries in the Partial Ligation Model

The specificity of MB$_{JAM-A}$ binding was confirmed 2 weeks after partial ligation by the absence of control nontargeted microbubbles retention and by competitive binding experiments using a 20-fold higher concentration of free anti–JAM-A antibody administered before MB$_{JAM-A}$ injection. Compared with normal binding conditions, blocking JAM-A leads to a reduction of MB$_{JAM-A}$ binding by 94% ($P=0.0008$).

The longitudinal assessment of JAM-A expression by molecular ultrasound revealed a slightly enhanced binding of MB$_{JAM-A}$ to the luminal side of the partially ligated carotid at 1 week post-ligation, followed by a strong increase after 2 weeks ($P=0.0009$). Subsequently, MB$_{JAM-A}$ binding decreased to a stable level at 3 ($P=0.0002$) and 4 ($P=0.0016$) weeks post-ligation (Figure 2A). Interestingly, JAM-A upregulation was also detected in the contralateral carotid 2 weeks after partial ligation ($P=0.028$), followed by a significant decrease in MB$_{JAM-A}$ binding at the 3 weeks time point ($P=0.02$) and a normalization 4 weeks post-intervention (Figure 2B). In sham-operated mice at 2 weeks post-intervention, the ultrasound signal generated by MB$_{JAM-A}$ was comparable to the mice before partial ligation, which indicates that the opening of the skin and the mobilization of the artery did not induce JAM-A translocation to the luminal surface of the endothelium.

Immunofluorescence of Carotid Arteries in the Partial Ligation Model

To determine the expression pattern and localization of JAM-A during endothelial activation and plaque development, JAM-A and platelet endothelial cell adhesion molecule 1 were stained at 1, 2, 3 and 4 weeks post-surgery (Figure 2C). One week after partial ligation of the left carotid artery, only focal areas
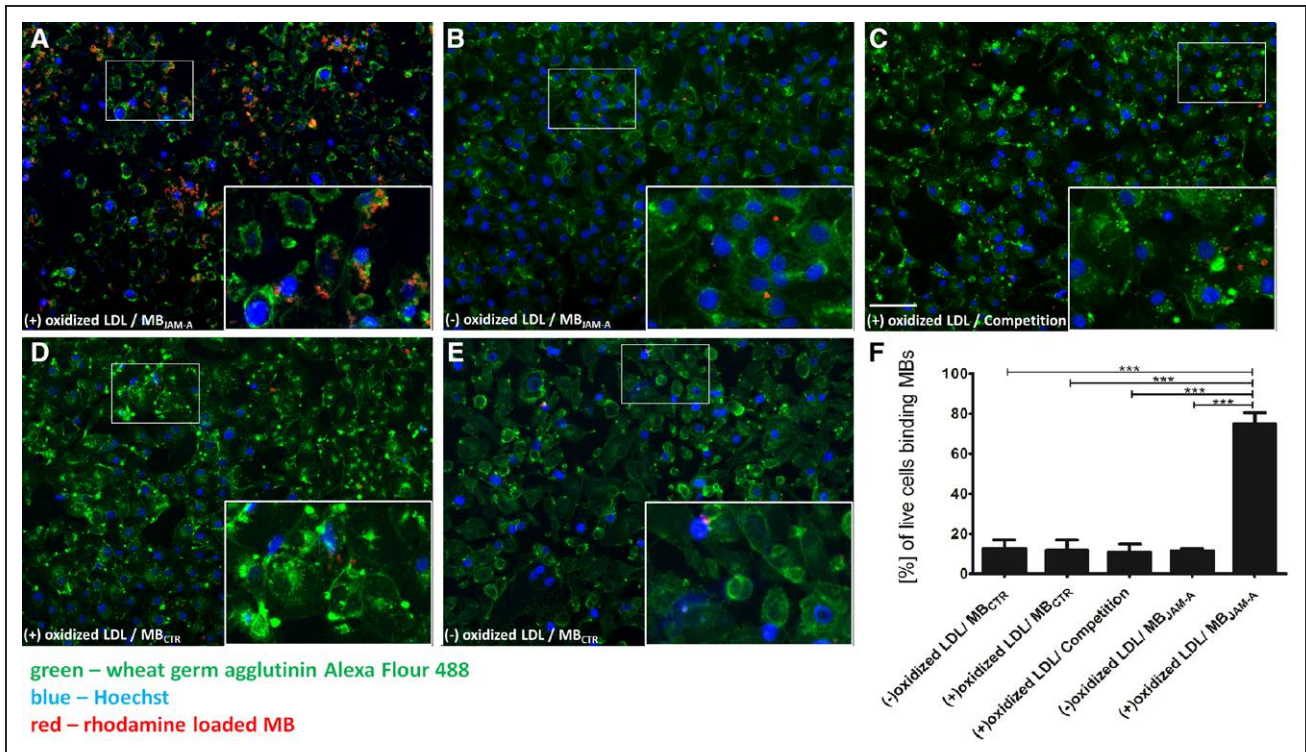
Figure 1. Binding affinity of junctional adhesion molecule A–targeted microbubbles (MB_{JAM-A}) in vitro. MB_{JAM-A} bound ≈7× more ($P<0.0001$) to stimulated human aortic endothelial cells (**A** and **F**) than to unstimulated cells (**B** and **F**) and ≈7× more ($P<0.0001$) than control nontargeted microbubbles (MB_{CTR}; **D** and **F**). There was no significant difference between the binding efficiency of MB_{CTR} (**E** and **F**) and MB_{JAM-A} (**B** and **F**) on unstimulated human aortic endothelial cells. The competitive binding studies (**C**) showed the specificity of MB_{JAM-A} to stimulated human aortic endothelial cells (scale bar, 100 µm). LDL indicates low-density lipoprotein.

of endothelia with JAM-A upregulation could be observed compared with sham animals. By week 2, JAM-A expression was strongly increased in both the endothelial and subendothelial layer, reaching a peak in luminal translocation.

Despite the lack of ligation (but in line with molecular ultrasound) also in the right carotid artery, an upregulation and luminal exposure of JAM-A were found 2 weeks after ligation of the left carotid artery (Figure 2D), which subsequently decreased reaching baseline levels 4 weeks post-surgery.

Morphological and Functional Measures of Arterial Remodeling in the Partial Ligation Model

To investigate the accompanying effects of JAM-A upregulation in both left and right carotid arteries, vascular wall thickness was quantified by ultrasound measurements. The vascular wall thickness in the ligated carotid artery continuously increased over the experimental period with most pronounced changes at the early time points (Figure 3A), indicating a progressive luminal stenosis (Figure 3B). Along with the plaque development and arterial narrowing, a decreased undulation of the vascular wall was observed, as shown by the quantification of lumen variation during systole and diastole (Figure 3C).

Interestingly, also in the contralateral carotid, a significant increase ($P<0.05$) in arterial wall thickness was observed 2 weeks after partial ligation, which, however, did not further progress at later time points (Figure 3D). In addition, this increase was not associated with a narrowing of the vessel

lumen (Figure 3E) or a change in arterial wall undulation during heart activity (data not shown).

Blood flow assessed by Doppler ultrasound was reduced by 56% to 69% over the timespan of 4 weeks in the left carotid artery post-ligation (Figure 4). As a compensatory response, the blood flow in the right carotid artery increased reaching a stable value after 3 weeks, suggesting a hemodynamic adjustment of the blood flow after partial ligation.

Inflammatory Serum Markers After Partial Ligation

To determine whether hemodynamic changes induce systemic inflammation and vascular vulnerability, inflammation markers and immune cell content of blood samples were quantified at different time points. The absolute numbers of leukocytes, neutrophils, monocytes, and lymphocytes did not significantly vary during the experiments (Table 1). Moreover, general inflammatory and anti-inflammatory markers, such as interferon γ, tumor necrosis factor α, granulocyte-macrophage colony-stimulating factor, interleukin-1b, -2, -4, -5, -6, -10, -12, -13, and -17, did not show significant changes in serum of the mice at any time point after partial ligation (Table 2), indicating the absence of systemic inflammatory condition.

JAM-A and Interleukin-6 Gene Expression in Carotid Arteries After Partial Ligation

Two weeks postpartial ligation, the JAM-A mRNA level in the ligated artery increased ($P<0.002$) when compared with
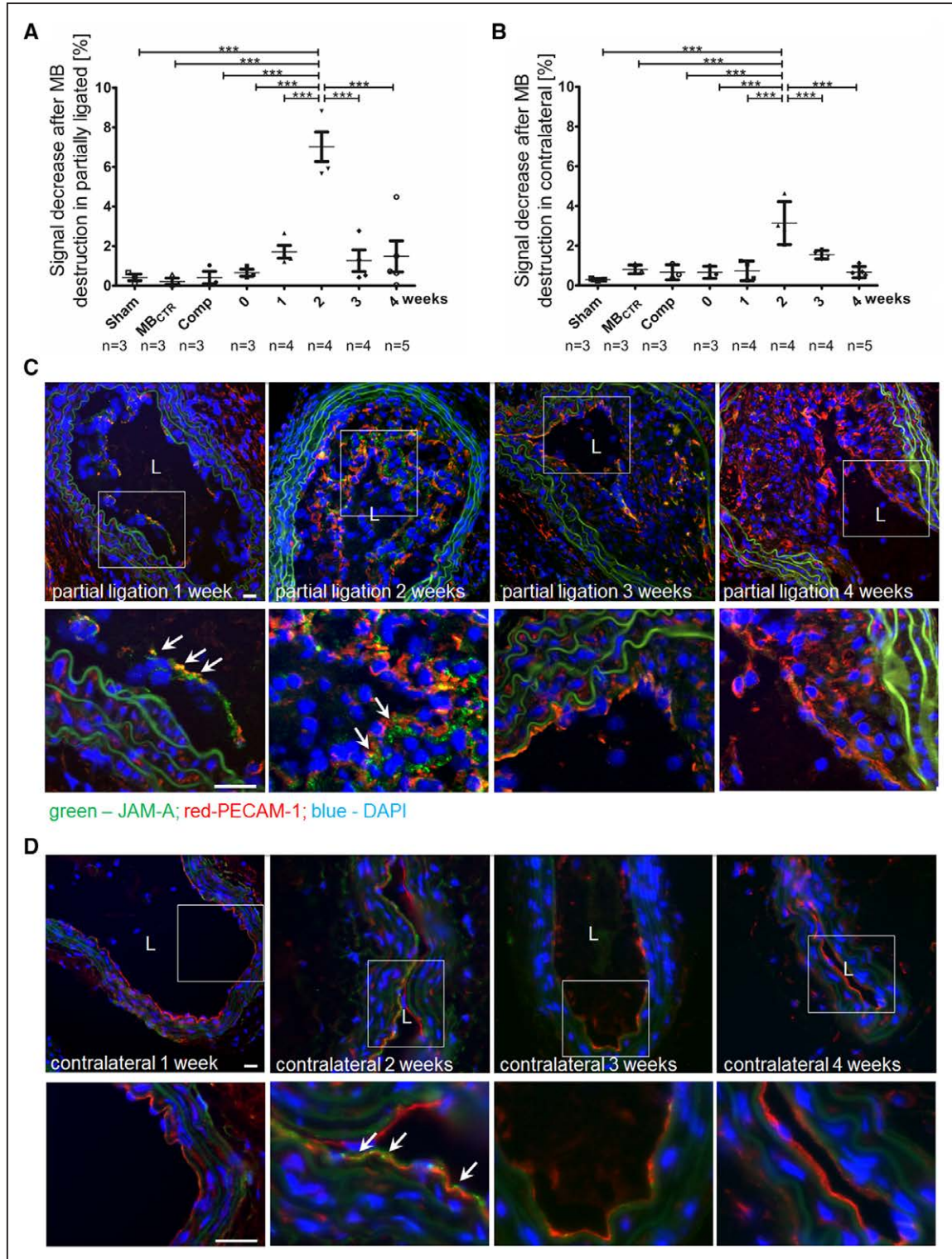
Figure 2. Quantification of junctional adhesion molecule A (JAM-A) after partial ligation. **A**, Ultrasound data analysis of JAM-A–targeted microbubbles (MB$_{JAM-A}$) binding in the partially ligated artery (n=23) compared with control (pre-operation) and competition (Comp) conditions. The MB$_{JAM-A}$ binding in the left partially ligated carotid artery reaches a peak after 2 wk followed by a rapid decline (****$P<0.001$). **B**, The corresponding ultrasound signal detected in the contralateral artery (n=23) indicated also a transient increase of MB$_{JAM-A}$ binding 2 wk post-partial ligation, which was also in line with the immunofluorescence (**$P<0.01$, ***$P<0.001$). MB adhesion assays were analyzed using the 1-way ANOVA followed by the Newman–Keuls post hoc-test. Error bars represent the SDs. **C**, Immunofluorescence staining of JAM-A (green) in the partially ligated carotid (arrows; n=4/time point) shows the expression of JAM-A on the surface of endothelial cells (stained with platelet endothelial cell adhesion molecule 1 [PECAM-1] in red). Nuclear counterstaining is performed with 4',6-diamidino-2-phenylindole (DAPI; blue). **D**, Immunofluorescence staining of JAM-A in the contralateral artery (n=4/time point). L marks the arterial lumen (scale bar, 20 μm). MB$_{CTR}$ indicates nontargeted control microbubbles.
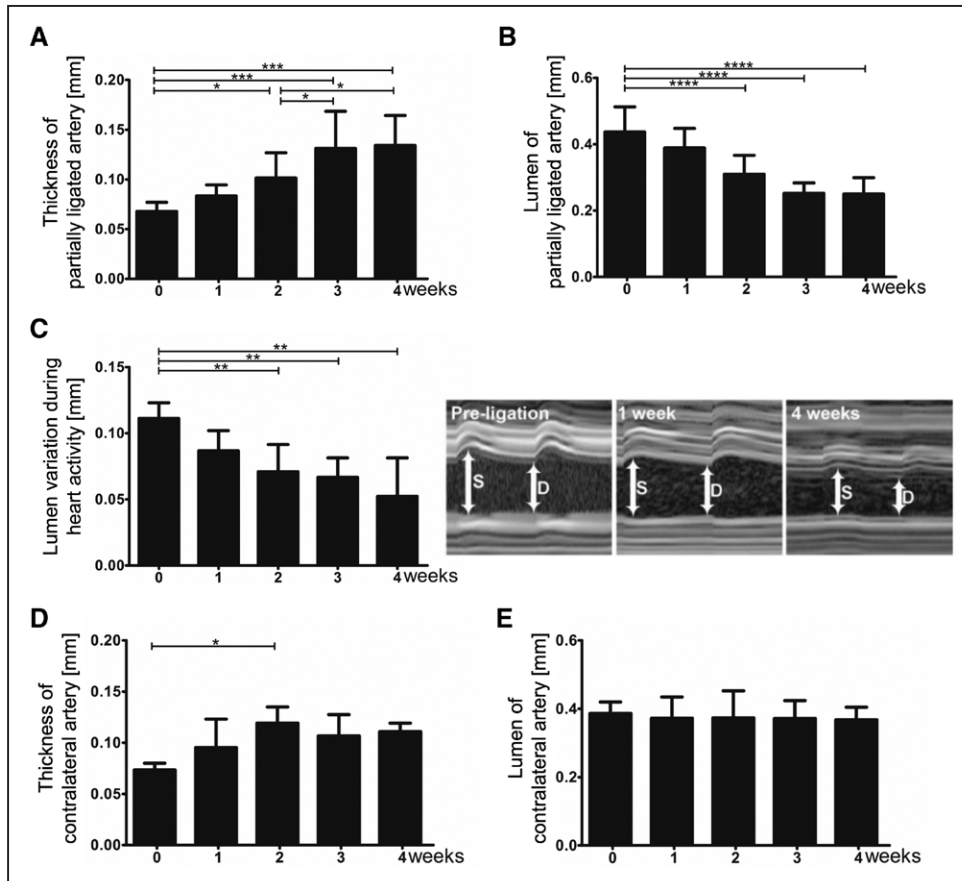
Figure 3. Arterial remodeling after partial ligation. **A**, Ultrasound quantification of vessel wall thickness (n=21, n=3–5/time point) revealed an initial significant increase 2 wk after partial ligation which peaks at later time points (*$P<0.05$; ***$P<0.001$). **B**, The early growth of an atherosclerotic plaque corresponds with a progressive luminal stenosis (****$P<0.001$). **C**, The undulation capacity of the vessel decreased progressively, along with the plaque development and arterial narrowing (**$P<0.01$). Representative M-mode images are shown, before surgery, 1 and 4 wk post-surgery, as indicated. White arrows indicate the lumen variation during systole (S) and diastole (D). **D**, Also in the contralateral carotid artery (n=21, n=3–5/time point), an increase in thickness of the arterial wall was observed 2 wk post-ligation (*$P<0.05$). However, the lumen of contralateral artery remained stable over the time of the experiment (**E**). Statistical significance was calculated using the 1-way ANOVA followed by the Newman–Keuls post hoc-test. Error bars represent the SDs.

JAM-A mRNA level measured before ligation (Figure 5A). The level of interleukin-6 increased ($P<0.001$) as well in the ligated carotid 2 weeks post-ligature (Figure 5B).

Discussion

In this study, we used JAM-A–targeted poly(n-butyl cyanoacrylate) microbubbles as contrast agents for molecular
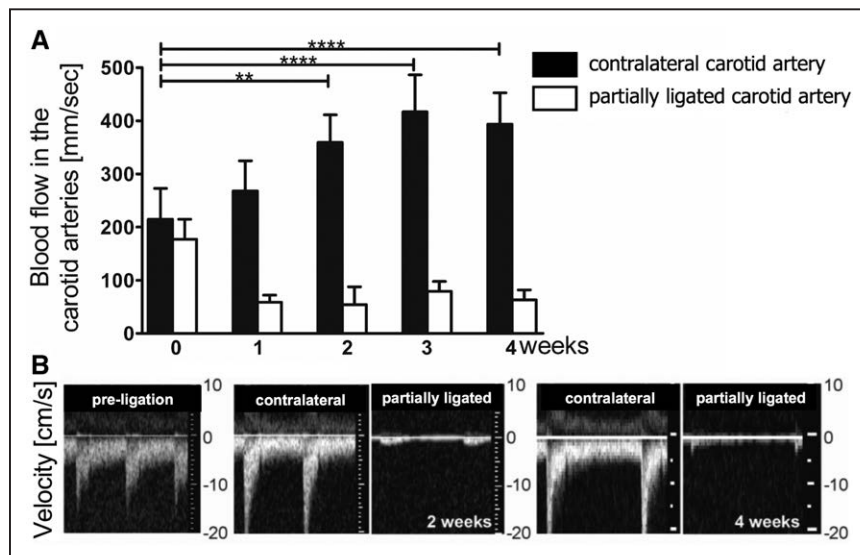
Figure 4. Blood flow hemodynamic after partial ligation. **A**, Blood flow is reduced in the partially ligated artery (white bars) while blood flow in the contralateral artery adjusts progressively to a higher velocity, stabilizing after 3 wk (**$P<0.01$; ****$P<0.001$; n=21, n=3–5/time point). Statistical significance was calculated using the 1-way ANOVA followed by the Newman–Keuls post hoc-test. Error bars represent the SDs. **B**, Representative ultrasound images of flow velocity in carotid arteries before, as well as 2 and 4 wk after partial ligation.

Table 1.   Immune Cells in Blood at Different Time Points After Partial Ligation

Cell Type	Before Surgery (n=4)	After Partial Ligation				P Value
		1 wk (n=4)	2 wk (n=4)	3 wk (n=4)	4 wk (n=4)	
Leukocytes ($\times 10^3/\mu$L)	8.0±1.9	6.5±1.2	6.4±1.7	7.9±1.4	6.2±1.3	n.s.
Neutrophils (%)	14±2.2	18±6.7	13±2.4	17±3.9	13±2.7	n.s.
Monocytes (%)	4.8±1.3	5.2±1.3	4.7±0.9	5.2±1.5	3.0±1.4	n.s.
Lymphocytes (%)	76±2.7	71±5.5	75±2.5	72±4.1	79±0.9	n.s.

n.s. indicates nonsignificant.

ultrasound imaging to identify early inflammatory endothelial sites which may develop toward atherosclerotic areas. The luminal availability of JAM-A significantly increased on the endothelium after acute decrease in blood flow in the left carotid artery because of partial ligation. As a result of the flow alteration in the ligated artery and local inflammation, atherosclerotic plaque growth was induced, leading to progressive lumen narrowing. Moreover, atherosclerotic lesion formation was associated with an increase in vascular wall thickness and a decrease in vascular wall undulations during systole and diastole, resembling the characteristics of atherosclerotic vessels in humans. The altered undulation of the artery points to a decreased vascular elasticity resulting from atherosclerotic plaque development and the change in matrix deposition to a high content of elastin. Both the thick cell-rich atherosclerotic plaque with multiple 4',6-diamidino-2-phenylindole–stained layers covering the internal elastic lamina and the increased autofluorescence of the elastic laminas because of the higher content of elastin[33] could be observed in the histological slides.

Decreased perfusion and oscillatory flow[3] represent a major local risk for the development and stability[34] of atherosclerotic lesions, and they also induce a low-level inflammatory state.[35] The onset of plaque growth and endothelial activation was sensitively detected using MB_{JAM-A} 2 weeks after vessel ligation. Although mRNA levels of the systemic inflammatory marker interleukin-6 increased 2 weeks post-partial ligation, no changes were found in the serum over the entire timeframe of the experiment. Therefore, we conclude that the inflammation was locally restricted. Our results are in line with other studies identifying the 2 weeks time period as the biologically active time window in the development of flow-induced endothelial dysfunction toward atherosclerosis.[36,37] However, the study of Schmitt et al[27] reports an upregulation of junctional JAM-A for an experimental period of 8 weeks. The prolonged upregulation of junctional JAM-A would be interesting to be detected with regular clinical diagnostic modalities and then correlate the results with clinical implications. Although, junctional JAM-A cannot be evaluated by molecular ultrasound using microbubbles because the latter are too big to penetrate into the junctional site of the endothelium. The microbubble size only allows the visualization of biological markers exposed to the luminal side of the endothelial cells. Therefore, this advantage of was recently used by Zhang et al[26] to describe the JAM-A upregulation by the endothelium covering vulnerable atherosclerotic plaques.

Because of the sudden blood flow restriction in the partially ligated left carotid artery, a redistribution of blood flow through the right carotid artery occurs.[38,39] This leads to

Table 2.   Serum Markers at Different Time Points After Partial Ligation

Serum Marker	Before Surgery (n=4)	After Partial Ligation				P Value
		1 wk (n=4)	2 wk (n=4)	3 wk (n=4)	4 wk (n=4)	
IFN-γ	0.2±0.3	0.0±0.0	1.7±3.4	0.0±0.0	0.0±0.1	n.s.
TNF-α	0.4±0.5	0.1±0.1	0.2±0.1	0.5±0.9	0.5±0.3	n.s.
GM-CSF	0.4±0.1	0.3±0.1	0.2±0.1	0.5±0.3	0.3±0.1	n.s.
IL-1b	5.0±8.1	1.3±1.7	3.0±4.9	13.9±22.2	3.7±7.4	n.s.
IL-2	0.0±0.0	0.0±0.0	0.0±0.0	0.9±1.9	0.1±0.3	n.s.
IL-4	5.9±7.9	0.0±0.0	0.0±0.0	12.8±25.6	3.3±6.6	n.s.
IL-5	1.8±1.9	2.4±0.5	1.3±0.8	2.1±2.3	3.2±4.3	n.s.
IL-6	7.0±8.9	7.3±6.3	8.6±8.1	15.8±24.7	14.6±15.8	n.s.
IL-10	7.9±8.5	12.5±17.5	2.7±4.9	10.7±19.0	16.0±21.3	n.s.
IL-12	2.3±3.7	0.9±1.6	0.9±1.9	8.7±12.2	3.6±2.8	n.s.
IL-13	3.3±6.6	5.0±10.0	0.0±0.0	24.2±48.4	0.0±0.0	n.s.
IL-17	3.6±4.4	0.0±0.0	0.0±0.0	1.8±3.1	3.6±4.9	n.s.

GM-CSF indicates granulocyte-macrophage colony-stimulating factor; IFN, interferon; IL, interleukin; n.s., nonsignificant; and TNF, tumor necrosis factor.
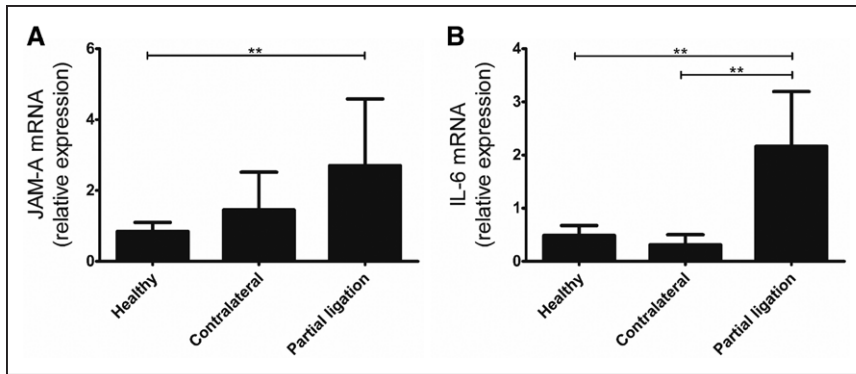
Figure 5. Junctional adhesion molecule A (JAM-A) and interleukin-6 (IL-6) gene expression in the carotid arteries 2 wk post-partial ligation. Both the JAM-A (**A**) and the IL-6 (**B**) levels were increased in the ligated carotid arteries 2 wk post-ligature. In the contralateral carotid, no significant increase of mRNA levels was identified. Statistical significance was calculated using the 1-way ANOVA followed by the Newman–Keuls post hoc-test. Error bars represent the SDs.

a higher perfusion in this vessel, which is accompanied by an increased pressure and shear stress. Although we did not observe a dilatation of the lumen in the right carotid artery, we found a compensatory thickening of the arterial wall as an adaptation mechanism to the increased pressure. It has already been described by Caro et al[40] that high wall shear stress has an atheroprotective role but that a sudden change in flow determining the oscillatory shear stress[41] after partial ligation is the promotor of atherosclerosis. This explains our findings in the contralateral carotid artery, where an acute increase in blood flow from normal state to a high state induces a transitory endothelial dysfunction which was faithfully detected with MB_{JAM-A} (2 weeks postpartial ligation) until the adaptation mechanisms was completed (3 weeks postpartial ligation). This hypothesis is further supported by the lack of elevated systemic inflammatory markers in the serum that would suggest a systemic inflammatory reaction. Thus, we postulate that endothelial cells are able to react toward temporal shear stress fluctuations[35,42] but also to adapt when the blood flow stabilizes.[42] In this context, JAM-A expression and imaging faithfully depict the biochemical changes taking place at the endothelial level, highlighting the potential of JAM-A as a versatile biochemical marker for endothelial activation. By using JAM-A as a biomarker to assess early stages of atherosclerotic plaque formation, molecular ultrasound using MB_{JAM-A} may enable the delineation of predisposed areas of atherosclerotic plaque development and the alternation in the onset and remission of atherosclerosis. The advantage of molecular ultrasound is that echography is a radiation-free, real-time, cheap, and broadly available diagnostic imaging modality. The imaging protocol could be applied to patients with cardiovascular disease who experience repeated paroxysmic high blood pressure episodes to detect acute activation of atherosclerosis-prone sites, and to adapt the medication accordingly, to thereby overcome worsening episodes of the cardiovascular disease.

Despite these promising results, there is still optimization required for the molecular ultrasound method. On the one hand, because of the short circulation time and high flow conditions, the unspecific binding of the microbubbles to the glycocalyx or their internalization by macrophages is low.[43] On the other hand, short circulation times limit the time span during which microbubbles can bind to their target. In addition, because of the physiological high flow conditions in the arteries, the retention of microbubbles at the target is relatively

short, which can make it difficult to investigate larger vessel areas by ultrasound. However, compared with our study in mice, a clinical setup would benefit from the larger vessel diameters, the higher vessel surface area, and the slower arterial flow. In addition, by using smaller targeting moieties and by increasing the number of targeting ligands on the microbubble surface, for example, by microbubble shell functionalization with dendrimeric spacers,[44] the target affinity and binding strength of microbubbles could be improved.

Although the applicability of ultrasound is limited to segmental body imaging, other imaging modalities, such as positron emission tomography, single-photon emission computed tomography, and magnetic resonance imaging, could be applied for whole body screening for predilection sites of atherosclerosis. In this context, JAM-A–targeted probes for positron emission tomography, single-photon emission computed tomography, and magnetic resonance imaging could be easily generated using the same binding moiety, thus highlighting the broad scope of the presented molecular imaging approach.

In conclusion, we demonstrate that noninvasive molecular ultrasound with MB_{JAM-A} is capable of detecting focal areas of transient endothelial activation triggered by the oscillatory blood flow condition. Thus, molecular ultrasound with MB_{JAM-A} may have the capacity to indicate predisposed areas of atherosclerotic plaque development, the onset of atherosclerosis, and its normalization during therapy.

Disclosures

None.

References

1. Kumar S, Kim CW, Simmons RD, Jo H. Role of flow-sensitive microRNAs in endothelial dysfunction and atherosclerosis: mechanosensitive athero-miRs. *Arterioscler Thromb Vasc Biol*. 2014;34:2206–2216. doi: 10.1161/ATVBAHA.114.303425.

2. Liehn EA, Zernecke A, Postea O, Weber C. Chemokines: inflammatory mediators of atherosclerosis. *Arch Physiol Biochem*. 2006;112:229–238. doi: 10.1080/13813450601093583.

3. Peiffer V, Sherwin SJ, Weinberg PD. Does low and oscillatory wall shear stress correlate spatially with early atherosclerosis? A systematic review. *Cardiovasc Res*. 2013;99:242–250. doi: 10.1093/cvr/cvt044.

4. Cecchi E, Giglioli C, Valente S, Lazzeri C, Gensini GF, Abbate R, Mannini L. Role of hemodynamic shear stress in cardiovascular disease. *Atherosclerosis*. 2011;214:249–256. doi: 10.1016/j.atherosclerosis.2010.09.008.

5. Rodondi N, Marques-Vidal P, Butler J, Sutton-Tyrrell K, Cornuz J, Satterfield S, Harris T, Bauer DC, Ferrucci L, Vittinghoff E, Newman AB; Health, Aging, and Body Composition Study. Markers of atherosclerosis and inflammation for prediction of coronary heart disease in older adults. *Am J Epidemiol*. 2010;171:540–549. doi: 10.1093/aje/kwp428.

6. Pagoto A, Stefania R, Garello F, Arena F, Digilio G, Aime S, Terreno E. Paramagnetic phospholipid-based micelles targeting VCAM-1 receptors for MRI visualization of inflammation. *Bioconjug Chem*. 2016;27:1921–1930. doi: 10.1021/acs.bioconjchem.6b00308.

7. Kaufmann BA, Carr CL, Belcik JT, Xie A, Yue Q, Chadderdon S, Caplan ES, Khangura J, Bullens S, Bunting S, Lindner JR. Molecular imaging of the initial inflammatory response in atherosclerosis: implications for early detection of disease. *Arterioscler Thromb Vasc Biol*. 2010;30:54–59. doi: 10.1161/ATVBAHA.109.196386.

8. Curaj A, Wu Z, Fokong S, Liehn EA, Weber C, Burlacu A, Lammers T, van Zandvoort M, Kiessling F. Noninvasive molecular ultrasound monitoring of vessel healing after intravascular surgical procedures in a preclinical setup. *Arterioscler Thromb Vasc Biol*. 2015;35:1366–1373. doi: 10.1161/ATVBAHA.114.304857.

9. Abou-Elkacem L, Bachawal SV, Willmann JK. Ultrasound molecular imaging: moving toward clinical translation. *Eur J Radiol*. 2015;84:1685–1693. doi: 10.1016/j.ejrad.2015.03.016.

10. Rix A, Fokong S, Heringer S, Pjontek R, Kabelitz L, Theek B, Brockmann MA, Wiesmann M, Kiessling F. Molecular ultrasound imaging of αvβ3-integrin expression in carotid arteries of pigs after vessel injury. *Invest Radiol*. 2016;51:767–775. doi: 10.1097/RLI.0000000000000282.

11. Wu Z, Curaj A, Fokong S, Liehn EA, Weber C, Lammers T, Kiessling F, Zandvoort van M. Rhodamine-loaded intercellular adhesion molecule-1-targeted microbubbles for dual-modality imaging under controlled shear stresses. *Circ Cardiovasc Imaging*. 2013;6:974–981. doi: 10.1161/CIRCIMAGING.113.000805.

12. Nahrendorf M, Keliher E, Panizzi P, Zhang H, Hembrador S, Figueiredo JL, Aikawa E, Kelly K, Libby P, Weissleder R. 18F-4V for PET-CT imaging of VCAM-1 expression in atherosclerosis. *JACC Cardiovasc Imaging*. 2009;2:1213–1222. doi: 10.1016/j.jcmg.2009.04.016.

13. Collins RG, Velji R, Guevara NV, Hicks MJ, Chan L, Beaudet AL. P-Selectin or intercellular adhesion molecule (ICAM)-1 deficiency substantially protects against atherosclerosis in apolipoprotein E-deficient mice. *J Exp Med*. 2000;191:189–194.

14. Daeichin V, Kooiman K, Skachkov I, Bosch JG, Theelen TL, Steiger K, Needles A, Janssen BJ, Daemen MJ, van der Steen AF, de Jong N, Sluimer JC. Quantification of endothelial αvβ3 expression with high-frequency ultrasound and targeted microbubbles: in vitro and in vivo studies. *Ultrasound Med Biol*. 2016;42:2283–2293. doi: 10.1016/j.ultrasmedbio.2016.05.005.

15. Calcagno C, Fayad ZA. Imaging the permeable endothelium: predicting plaque rupture in atherosclerotic rabbits. *Circ Cardiovasc Imaging*. 2016;9:e005955. doi: 10.1161/CIRCIMAGING.116.005955.

16. Gargiulo S, Gramanzini M, Mancini M. Molecular imaging of vulnerable atherosclerotic plaques in animal models. *Int J Mol Sci*. 2016;17:1511–1555.

17. Toczek J, Sadeghi MM. A new tracer for imaging atherosclerosis. *Circ Cardiovasc Imaging*. 2016;9:e004889. doi: 10.1161/CIRCIMAGING.116.004889.

18. Wang X, Peter K. Molecular imaging of atherothrombotic diseases: seeing is believing. *Arterioscler Thromb Vasc Biol*. 2017;37:1029–1040. doi: 10.1161/ATVBAHA.116.306483.

19. Calin M, Stan D, Schlesinger M, Simion V, Deleanu M, Constantinescu CA, Gan AM, Pirvulescu MM, Butoi E, Manduteanu I, Bota M, Enachescu M, Borsig L, Bendas G, Simionescu M. VCAM-1 directed target-sensitive liposomes carrying CCR2 antagonists bind to activated endothelium and reduce adhesion and transmigration of monocytes. *Eur J Pharm Biopharm*. 2015;89:18–29. doi: 10.1016/j.ejpb.2014.11.016.

20. Davies MJ, Gordon JL, Gearing AJ, Pigott R, Woolf N, Katz D, Kyriakopoulos A. The expression of the adhesion molecules ICAM-1, VCAM-1, PECAM, and E-selectin in human atherosclerosis. *J Pathol*. 1993;171:223–229. doi: 10.1002/path.1711710311.

21. Lindner V, Collins T. Expression of NF-kappa B and I kappa B-alpha by aortic endothelium in an arterial injury model. *Am J Pathol*. 1996;148:427–438.

22. Zeiffer U, Schober A, Lietz M, Liehn EA, Erl W, Emans N, Yan ZQ, Weber C. Neointimal smooth muscle cells display a proinflammatory phenotype resulting in increased leukocyte recruitment mediated by P-selectin and chemokines. *Circ Res*. 2004;94:776–784. doi: 10.1161/01.RES.0000121105.72718.5C.

23. Kennedy S, McPhaden AR, Wadsworth RM, Wainwright CL. Correlation of leukocyte adhesiveness, adhesion molecule expression and leukocyte-induced contraction following balloon angioplasty. *Br J Pharmacol*. 2000;130:95–103. doi: 10.1038/sj.bjp.0703282.

24. Videm V, Albrigtsen M. Soluble ICAM-1 and VCAM-1 as markers of endothelial activation. *Scand J Immunol*. 2008;67:523–531. doi: 10.1111/j.1365-3083.2008.02029.x.

25. Deshpande N, Needles A, Willmann JK. Molecular ultrasound imaging: current status and future directions. *Clin Radiol*. 2010;65:567–581. doi: 10.1016/j.crad.2010.02.013.

26. Zhang YJ, Bai DN, Du JX, Jin L, Ma J, Yang JL, Cai WB, Feng Y, Xing CY, Yuan LJ, Duan YY. Ultrasound-guided imaging of junctional adhesion molecule-A-targeted microbubbles identifies vulnerable plaque in rabbits. *Biomaterials*. 2016;94:20–30. doi: 10.1016/j.biomaterials.2016.03.049.

27. Schmitt MM, Megens RT, Zernecke A, Bidzhekov K, van den Akker NM, Rademakers T, van Zandvoort MA, Hackeng TM, Koenen RR, Weber C. Endothelial junctional adhesion molecule-a guides monocytes into flow-dependent predilection sites of atherosclerosis. *Circulation*. 2014;129:66–76. doi: 10.1161/CIRCULATIONAHA.113.004149.

28. Ostermann G, Weber KS, Zernecke A, Schröder A, Weber C. JAM-1 is a ligand of the beta(2) integrin LFA-1 involved in transendothelial migration of leukocytes. *Nat Immunol*. 2002;3:151–158. doi: 10.1038/ni755.

29. Bazzoni G. The JAM family of junctional adhesion molecules. *Curr Opin Cell Biol*. 2003;15:525–530.

30. Schmitt MM, Fraemohs L, Hackeng TM, Weber C, Koenen RR. Atherogenic mononuclear cell recruitment is facilitated by oxidized lipoprotein-induced endothelial junctional adhesion molecule-A redistribution. *Atherosclerosis*. 2014;234:254–264. doi: 10.1016/j.atherosclerosis.2014.03.014.

31. Zernecke A, Liehn EA, Fraemohs L, von Hundelshausen P, Koenen RR, Corada M, Dejana E, Weber C. Importance of junctional adhesion molecule-A for neointimal lesion formation and infiltration in atherosclerosis-prone mice. *Arterioscler Thromb Vasc Biol*. 2006;26:e10–e13. doi: 10.1161/01.ATV.0000197852.24529.4f.

32. Chang CH, Hale SJ, Cox CV, Blair A, Kronsteiner B, Grabowska R, Zhang Y, Cook D, Khoo CP, Schrader JB, Kabuga SB, Martin-Rendon E, Watt SM. Junctional adhesion molecule-A is highly expressed on human hematopoietic repopulating cells and associates with the key hematopoietic chemokine receptor CXCR4. *Stem Cells*. 2016;34:1664–1678. doi: 10.1002/stem.2340.

33. Makowski MR, Wiethoff AJ, Blume U, Cuello F, Warley A, Jansen CH, Nagel E, Razavi R, Onthank DC, Cesati RR, Marber MS, Schaeffter T, Smith A, Robinson SP, Botnar RM. Assessment of atherosclerotic plaque burden with an elastin-specific magnetic resonance contrast agent. *Nat Med*. 2011;17:383–388. doi: 10.1038/nm.2310.

34. Gorog DA, Fayad ZA, Fuster V. Arterial thrombus stability: does it matter and can we detect it? *J Am Coll Cardiol*. 2017;70:2036–2047. doi: 10.1016/j.jacc.2017.08.065.

35. Davies PF, Civelek M, Fang Y, Fleming I. The atherosusceptible endothelium: endothelial phenotypes in complex haemodynamic shear stress regions in vivo. *Cardiovasc Res*. 2013;99:315–327. doi: 10.1093/cvr/cvt101.

36. Singla DK, Singla R, Wang J. BMP-7 treatment increases M2 macrophage differentiation and reduces inflammation and plaque formation in Apo E-/- mice. *PLoS One*. 2016;11:e0147897. doi: 10.1371/journal.pone.0147897.

37. Shin IJ, Shon SM, Schellingerhout D, Park JY, Kim JY, Lee SK, Lee DK, Lee HW, Ahn BC, Kim K, Kwon IC, Kim DE. Characterization of partial ligation-induced carotid atherosclerosis model using dual-modality molecular imaging in ApoE knock-out mice. *PLoS One*. 2013;8:e73451. doi: 10.1371/journal.pone.0073451.

38. Korshunov VA, Berk BC. Flow-induced vascular remodeling in the mouse: a model for carotid intima-media thickening. *Arterioscler Thromb Vasc Biol*. 2003;23:2185–2191. doi: 10.1161/01.ATV.0000103120.06092.14.

39. Sullivan CJ, Hoying JB. Flow-dependent remodeling in the carotid artery of fibroblast growth factor-2 knockout mice. *Arterioscler Thromb Vasc Biol*. 2002;22:1100–1105.

40. Caro CG, Fitz-Gerald JM, Schroter RC. Atheroma and arterial wall shear. Observation, correlation and proposal of a shear dependent mass transfer mechanism for atherogenesis. *Proc R Soc Lond B Biol Sci*. 1971;177:109–159.

41. Ku DN, Giddens DP, Zarins CK, Glagov S. Pulsatile flow and atherosclerosis in the human carotid bifurcation. Positive correlation between plaque location and low oscillating shear stress. *Arteriosclerosis*. 1985;5:293–302.

42. Davies PF, Dewey CF Jr, Bussolari SR, Gordon EJ, Gimbrone MA Jr. Influence of hemodynamic forces on vascular endothelial function. *In vitro* studies of shear stress and pinocytosis in bovine aortic cells. *J Clin Invest*. 1984;73:1121–1129. doi: 10.1172/JCI111298.

43. Bioley G, Bussat P, Lassus A, Schneider M, Terrettaz J, Corthésy B. The phagocytosis of gas-filled microbubbles by human and murine antigen-presenting cells. *Biomaterials*. 2012;33:333–342. doi: 10.1016/j.biomaterials.2011.09.045.

44. Barge A, Caporaso M, Cravotto G, Martina K, Tosco P, Aime S, Carrera C, Gianolio E, Pariani G, Corpillo D. Design and synthesis of a $\gamma(1)\beta(8)$-cyclodextrin oligomer: a new platform with potential application as a dendrimeric multicarrier. *Chemistry*. 2013;19:12086–12092. doi: 10.1002/chem.201301215.

Highlights

- Junctional adhesion molecule A (JAM-A) expression can faithfully be imaged using molecularly targeted ultrasound imaging.
- Acute blood flow fluctuations in healthy arteries induce transitory endothelial dysfunction leading to temporary JAM-A expression, which can be detected with JAM-A–targeted microbubbles.
- JAM-A is a valuable imaging biomarker to assess endothelial activation and dysfunction at early and even reversible stages.
- JAM-A is suggested as a valuable imaging biomarker to assess early stages of atherosclerotic plaque formation.